




# Loss of adipose TET proteins enhances $\beta$ -adrenergic responses and protects against obesity by epigenetic regulation of $\beta$ 3-AR expression

Seongjun Byun<sup>a,1</sup>, Chan Hyeong Lee<sup>b,1</sup>, Hyeongmin Jeong<sup>a,1</sup>, Hyejin Kim<sup>a</sup>, Hyug Moo Kwon<sup>a</sup>, Sungho Park<sup>a</sup>, Kyungjae Myung<sup>c,d</sup> , Jungeun An<sup>b,2</sup>, and Myunggon Ko<sup>a,d,2</sup>

Edited by C. Ronald Kahn, Harvard Medical School, Boston, MA; received April 6, 2022; accepted April 25, 2022

$\beta$ -adrenergic receptor ( $\beta$ -AR) signaling plays predominant roles in modulating energy expenditure by triggering lipolysis and thermogenesis in adipose tissue, thereby conferring obesity resistance. Obesity is associated with diminished  $\beta$ 3-adrenergic receptor ( $\beta$ 3-AR) expression and decreased  $\beta$ -adrenergic responses, but the molecular mechanism coupling nutrient overload to catecholamine resistance remains poorly defined. Ten-eleven translocation (TET) proteins are dioxygenases that alter the methylation status of DNA by oxidizing 5-methylcytosine to 5-hydroxymethylcytosine and further oxidized derivatives. Here, we show that TET proteins are pivotal epigenetic suppressors of  $\beta$ 3-AR expression in adipocytes, thereby attenuating the responsiveness to  $\beta$ -adrenergic stimulation. Deletion of all three *Tet* genes in adipocytes led to increased  $\beta$ 3-AR expression and thereby enhanced the downstream  $\beta$ -adrenergic responses, including lipolysis, thermogenic gene induction, oxidative metabolism, and fat browning in vitro and in vivo. In mouse adipose tissues, *Tet* expression was elevated after mice ate a high-fat diet. Mice with adipose-specific ablation of all TET proteins maintained higher levels of  $\beta$ 3-AR in both white and brown adipose tissues and remained sensitive to  $\beta$ -AR stimuli under high-fat diet challenge, leading to augmented energy expenditure and decreased fat accumulation. Consequently, they exhibited improved cold tolerance and were substantially protected from diet-induced obesity, inflammation, and metabolic complications, including insulin resistance and hyperlipidemia. Mechanistically, TET proteins directly repressed  $\beta$ 3-AR transcription, mainly in an enzymatic activity-independent manner, and involved the recruitment of histone deacetylases to increase deacetylation of its promoter. Thus, the TET–histone deacetylase– $\beta$ 3-AR axis could be targeted to treat obesity and related metabolic diseases.

TET proteins |  $\beta$ 3-AR | catecholamine resistance | obesity | HDACs

Beta-adrenergic signaling is a crucial modulator of energy expenditure that triggers lipolysis and heat dissipation in brown and beige adipocytes (1, 2). Upon cold exposure, sympathetic nerve terminals release the catecholamines norepinephrine and epinephrine, which bind to  $\beta$ -adrenergic receptors ( $\beta$ -ARs) and activate the intracellular signaling cascade involving adenylyl cyclase/cyclic adenosine monophosphate (cAMP)/protein kinase A (PKA) (3, 4). This event ultimately triggers hydrolysis of stored triglycerides (TGs) by activating key lipases, including hormone-sensitive lipase (HSL). Fatty acids derived from lipolysis are transported to the mitochondria and consumed as fuels to produce thermal energy (1, 2). Furthermore, free fatty acids are proposed to be allosteric activators of uncoupling protein 1 (UCP1) (5). During adaptive thermogenesis,  $\beta$ -AR signals also activate key thermogenic genes, including *Ppargc1a* (encoding PPAR $\gamma$  coactivator-1 $\alpha$  [Pgc-1 $\alpha$ ]), *Ucp1*, and various components of the electron transport chain, thus promoting mitochondrial biogenesis, fatty acid oxidation, and thermogenesis (2–4). Additionally,  $\beta$ -ARs are important regulators of fat browning. There are three  $\beta$ -AR subtypes:  $\beta$ 1-,  $\beta$ 2-, and  $\beta$ 3-AR. In mice,  $\beta$ 3-AR plays important roles in inducing beige adipocytes from pre-existing white adipocytes in response to  $\beta$ -adrenergic agonists, whereas  $\beta$ 1-AR mainly mediates beige adipocyte generation following cold exposure (6).  $\beta$ 3-AR is also important for browning, lipolysis, and thermogenesis in human adipocytes (7, 8).

In addition to cold-induced thermogenesis,  $\beta$ -ARs also play essential roles in diet-induced thermogenesis. A Trp64Arg mutation in the  *$\beta$ 3-AR* gene is associated with abdominal obesity and increased susceptibility to weight gain and insulin resistance (9, 10). Mice lacking all three  $\beta$ -ARs subtypes (known as “ $\beta$ -less” mice) are prone to diet-induced obesity, due to a significantly lower metabolic rate (11). Strikingly, the brown adipose tissue (BAT) from  $\beta$ -less mice display white adipose tissue (WAT)-like features, mainly populated by markedly enlarged adipocytes with unilocular lipid

## Significance

The  $\beta$ 3-adrenergic receptor ( $\beta$ 3-AR) is a major regulator of energy expenditure that triggers lipolysis and thermogenesis in adipose tissue, thereby significantly attenuating the risk of obesity. Obesity is associated with diminished  $\beta$ 3-AR expression and decreased  $\beta$ -adrenergic responses, but the underlying molecular mechanisms remain elusive. Here, we show that ten-eleven translocation (TET) proteins, the crucial modifiers of DNA methylation, act as epigenetic suppressors of  $\beta$ 3-AR in adipocytes by recruiting histone deacetylases to its promoter, thereby reducing the sensitivity to  $\beta$ -adrenergic stimulation. Adipose-specific ablation of all TET proteins in mice prevents body weight gain and metabolic disorders under high-fat diet challenge via enhanced fat browning, lipolysis, and thermogenesis. Modulation of adipocyte TET proteins may provide a new therapeutic avenue to treat obesity.

Author contributions: S.B., C.H.L., H.J., H.K., J.A., and M.K. designed research; S.B., C.H.L., H.J., and J.A. performed research; H.M.K. and K.M. contributed new reagents/analytic tools; S.B., C.H.L., H.K., S.P., K.M., J.A., and M.K. analyzed data; and J.A. and M.K. wrote the paper.

The authors declare no competing interest.

This article is a PNAS Direct Submission.

Copyright © 2022 the Author(s). Published by PNAS. This article is distributed under Creative Commons Attribution-NonCommercial-NoDerivatives License 4.0 (CC BY-NC-ND).

<sup>1</sup>S.B., C.H.L., and H.J. contributed equally to this work.

<sup>2</sup>To whom correspondence may be addressed. Email: mgko@unist.ac.kr or jan@jbn.u.ac.kr.

This article contains supporting information online at <http://www.pnas.org/lookup/suppl/doi:10.1073/pnas.2205626119/-/DCSupplemental>.

Published June 23, 2022.

droplets that lack UCP1 expression. Consistently, the  $\beta$ -less mice are highly susceptible to cold-induced hypothermia and are unable to increase oxygen consumption in response to  $\beta$ -agonist treatment. Mice lacking  $\beta$ 3-AR alone are also susceptible to depositing more fat compared to wild-type (WT) mice (12). Notably, in both humans and rodents, obesity is associated with blunted  $\beta$ -AR-triggered responses in adipose tissue (AT), a state known as catecholamine resistance (13–15), presumably due to a significant reduction of  $\beta$ 3-AR expression and function in response to chronic nutrient overload (16–19). Furthermore,  $\beta$ -ARs, particularly  $\beta$ 1-AR and  $\beta$ 2-AR, undergo agonist-induced desensitization (20, 21). In rodents, selective  $\beta$ 3-AR agonists exert excellent antiobesity and antidiabetic effects by increasing energy expenditure, due to their abilities to induce lipolysis, mitochondrial biogenesis, fat oxidation, and the thermogenic program in AT (22–26). However, results of most clinical studies targeting  $\beta$ 3-AR have been disappointing (27), although mirabegron, a selective  $\beta$ 3-AR agonist approved for the treatment of overactive bladder syndrome (2), activated human brown and beige adipocytes and improved glucose metabolism in obese individuals when treated chronically or at high doses (7, 28–31). This might be attributed to the poor selectivity of the human  $\beta$ 3-AR agonists and different expression patterns of  $\beta$ -ARs in rodents and human ATs. Indeed,  $\beta$ 3-AR is abundantly expressed in both WAT and BAT in rodents and thus acts as the principal receptor of catecholamine signals. However, its levels are very low in human ATs. Instead,  $\beta$ -adrenergic stimulation of human adipocytes is mainly mediated by  $\beta$ 1-AR and  $\beta$ 2-AR, whose agonists often induce undesired complications, including hypertension and tachycardia (27). Together, these results strongly suggest that strategies to potentiate  $\beta$ 3-AR expression and catecholamine sensitivity with minimal side effects in AT may be promising in obesity treatments.

Ten-eleven translocation (TET) proteins are dioxygenases that reprogram or erase the methylation status of DNA by oxidizing 5-methylcytosine to 5-hydroxymethylcytosine (5hmC) and further oxidized derivatives (32). They are crucial regulators of gene expression that serve as either transcriptional activators or repressors, depending on the context (32, 33). In many cell types, including mouse embryonic stem cells, immune cells, or neuronal cells, TET proteins utilize their enzymatic activities to sequentially oxidize 5-methylcytosine to 5hmC and further oxidation products at promoters or enhancers, followed by DNA demethylation, to control gene transcription (34, 35). However, they can also control gene expression independently of their enzymatic activity, which is mainly achieved by partnering with numerous transcription factors and associated coregulators, including chromatin modifiers (36–39). For example, TET proteins can be implicated in the formation of transcriptional corepressor complex with histone deacetylase (HDAC) to repress transcription (37–39).

Previous studies have suggested that TET proteins may have regulatory roles in adipocyte differentiation and function. Depletion of TET1 or TET2 substantially inhibits adipogenic differentiation of 3T3-L1 preadipocytes or mouse embryonic fibroblasts (40, 41). However, a recent study showed that TET1 is dispensable for adipogenesis of primary preadipocytes isolated from mice (42). Moreover, in mature adipocytes, TET proteins are involved in the PPAR $\gamma$ -regulated transcriptional program by being recruited to PPAR $\gamma$  response elements and inducing their demethylation to activate PPAR $\gamma$  target genes (40). In mice, all three TET proteins are expressed in various adipose depots, although at different levels (39), and TET1 suppresses thermogenesis by repressing *Ucp1* and *Ppargc1a* in a beige adipocyte-specific manner (39). As a result, *Tet1* knockout

mice are cold tolerant and partially protected from diet-induced obesity and metabolic dysfunction. In contrast, another recent report showed that *Tet1* haploinsufficiency promotes diet-induced obesity and aggravates glucose intolerance (42). Thus, the exact roles of TET proteins in adipocyte biology and metabolism remain unclear.

We show here that chromatin modification via TET-HDAC interaction constitutes a crucial regulatory component of adipocyte plasticity and adaptive thermogenesis by modulating  $\beta$ 3-AR expression and catecholamine sensitivity. TET proteins acted as pivotal epigenetic suppressors of  $\beta$ 3-AR expression in adipocytes, thereby reducing the sensitivity to  $\beta$ -adrenergic stimulation in vitro and in vivo. Thus, TET loss resulted in enhanced  $\beta$ -adrenergic responses, including browning, lipolysis, thermogenic gene induction, mitochondrial respiration, and fatty acid oxidation. Moreover, mice lacking all TET proteins in adipocytes resisted  $\beta$ 3-AR down-regulation and remained sensitive to  $\beta$ -AR stimuli during chronic high-fat diet (HFD) challenge. Consequently, the knockout mice maintained a higher capacity for fat lipolysis, thermogenesis, and energy expenditure, and were substantially resistant to diet-induced obesity and associated metabolic complications.

## Results

**TET Deficiency Increases  $\beta$ -Adrenergic Responsiveness by Up-Regulating  $\beta$ 3-AR Expression in Adipocytes.** It was previously reported that TET1 directly repressed the expression of crucial thermogenic genes, including *Ucp1* and *Ppargc1a*, in beige adipocytes (39). As a result, its loss increased energy expenditure and partially protected mice from diet-induced obesity and related metabolic comorbidities.  $\beta$ 3-AR is the principal regulator of lipolysis and thermogenesis that acts upstream of *Ucp1* and *Ppargc1a* (1, 2). Thus, we aimed to investigate whether TET proteins could control the expression of  $\beta$ 3-ARs, thereby modulating  $\beta$ -adrenergic responsiveness to indirectly control the downstream thermogenic program. To test this, we established immortalized stromal vascular fraction cells isolated from the subcutaneous inguinal WAT (iWAT) of *Tet1<sup>fl/fl</sup> Tet2<sup>fl/fl</sup> Tet3<sup>fl/fl</sup> Cre-ERT2* mice (*SI Appendix, Fig. S1A*). All three *Tet* genes were successfully deleted after 48 h of 4-hydroxytamoxifen (4-OHT) treatment that activated the Cre-ERT2 recombinase (*SI Appendix, Fig. S1B*). Notably, deletion of all *Tet* genes at the early phase of adipogenic differentiation (achieved by treating preadipocytes with 4-OHT at day  $-3$  or day 0) almost completely blocked adipogenesis in vitro, as assessed by quantification of accumulated lipids and expression of adipogenic marker genes such as *Pparg* and *Fabp4* (*SI Appendix, Fig. S1 C–E*). However, *Tet* deletion at a later stage (achieved by treating cells with 4-OHT at day 2 of differentiation) did not significantly affect adipogenesis (*SI Appendix, Fig. S1 C–E*), thus indicating a stage-specific requirement for TET proteins in adipogenesis. Based on these results, we used WT and *Tet1*, *Tet2*, *Tet3* triple knockout (hereafter, *Tet* TKO) adipocytes under similar differentiation states for subsequent studies (Fig. 1A), where *Tet* deletion was also monitored by 5hmC loss using a dot blot assay (43) (Fig. 1B). Importantly, the  $\beta$ 3-AR mRNA and protein levels were significantly elevated in *Tet* TKO adipocytes (Fig. 1 C and D and *SI Appendix, Fig. S1F*). Among the three  $\beta$ -AR subtypes,  $\beta$ 3-AR up-regulation was most prominent upon *Tet* deletion (*SI Appendix, Fig. S1G*). As expected, both mRNA and protein levels of Pgc-1 $\alpha$  and *Ucp1* were also increased in *Tet* TKO adipocytes (Fig. 1 C and D).

Stimulation of  $\beta$ -ARs activates the cAMP/PKA signaling cascade that ultimately triggers lipolysis by activating key lipases, including HSL (1–4). Furthermore, activated  $\beta$ -ARs also stimulate the transcription of key thermogenic genes, including *Ppargc1a*, *Ucp1*, and various genes implicated in mitochondrial respiration

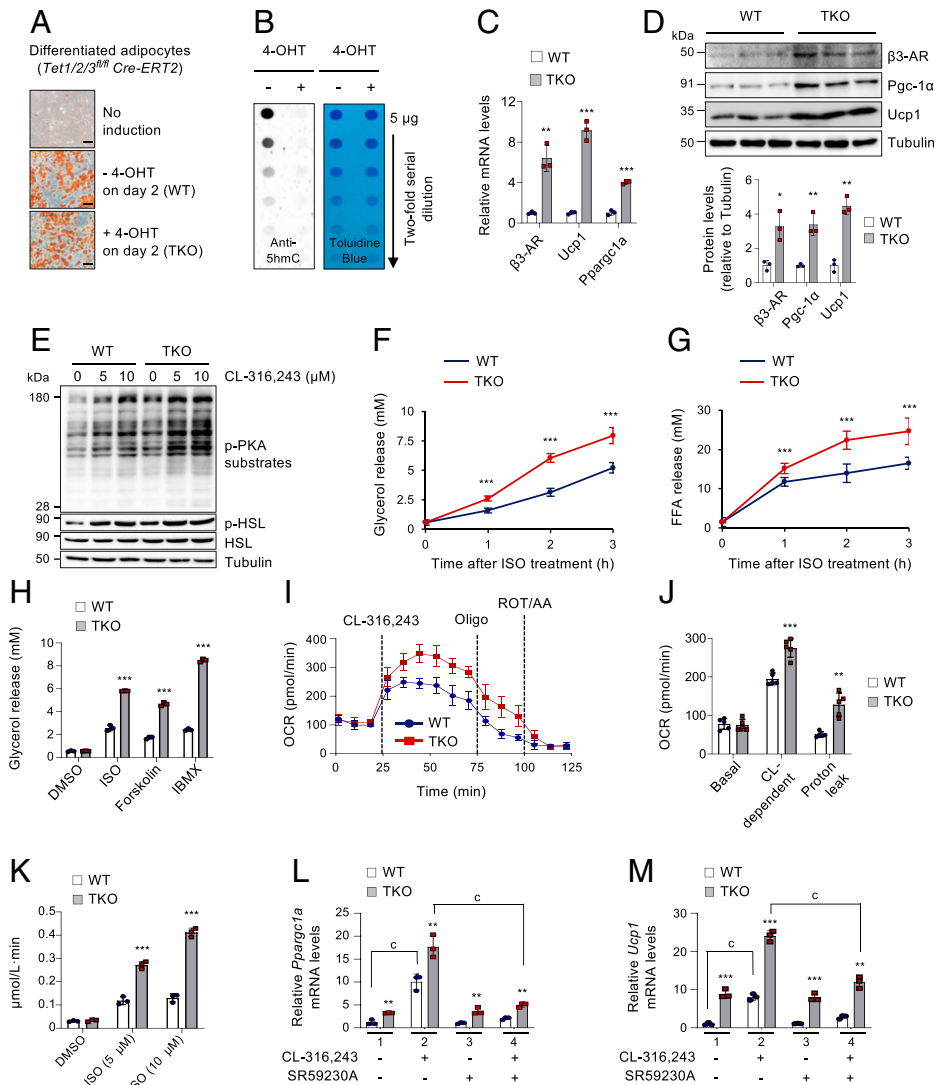


**Fig. 1.** TET deficiency increases  $\beta$ -adrenergic responsiveness by up-regulating  $\beta$ -AR expression in adipocytes. (A) Oil Red O staining of differentiated WT and *Tet* TKO adipocytes. Pre-adipocytes were treated with or without 4-OHT on day 2 of differentiation.  $n = 3$ . (Scale bar, 100  $\mu$ m.) (B) Dot blot analysis to quantify genomic 5hmC in WT and *Tet* TKO adipocytes shown in A. Toluidine blue staining confirmed blotting of equal amounts of DNA. (C) mRNA expression of  $\beta$ -AR, *Ucp1*, and *Pparg1a* relative to *Gapdh* in WT and *Tet* TKO adipocytes.  $n = 3$ . (D) Immunoblot analysis (Top) and quantification (Bottom) of  $\beta$ -AR, Pgc-1 $\alpha$ , and Ucp1 proteins in WT and *Tet* TKO adipocytes.  $\alpha$ -Tubulin served as a loading control.  $n = 3$ . (E) Immunoblot analysis of p-PKA substrates, p-HSL, and total HSL proteins in WT and *Tet* TKO adipocytes stimulated with or without CL-316,243 for 5 min at the indicated concentrations.  $\alpha$ -Tubulin served as a loading control. (F and G) In vitro lipolysis in WT and *Tet* TKO adipocytes. The released glycerol (F) and free fatty acid (G) were quantified at the indicated time points after stimulation with ISO (5  $\mu$ M).  $n = 3$ . (H) In vitro lipolysis in WT and *Tet* TKO adipocytes stimulated with ISO (5  $\mu$ M), forskolin (20  $\mu$ M), or isobutylmethylxanthine (IBMX) (0.2 mM).  $n = 3$ . (I and J) Oxygen consumption rate (OCR) (I) and average OCR (J) in WT and *Tet* TKO adipocytes sequentially stimulated with CL-316,243 (10  $\mu$ M), oligomycin (oligo; 1.25  $\mu$ M), and rotenone/antimycin A (ROT/AA, 1  $\mu$ M).  $n = 5$ . (K) In vitro fatty acid oxidation in WT and *Tet* TKO adipocytes stimulated with ISO at the indicated concentrations.  $n = 3$ . (L and M) mRNA expression of *Pparg1a* (L) and *Ucp1* (M) relative to *Gapdh* in WT and *Tet* TKO adipocytes stimulated with or without CL-316,243 (1  $\mu$ M, 24 h). Cells were either untreated or pretreated for 1 h with SR59230A (10  $\mu$ M), a  $\beta$ -AR antagonist, prior to CL-316,243 treatments.  $n = 3$ . All data are presented as the mean  $\pm$  SD. The  $P$  values were determined by unpaired Student's  $t$  test. \*\* $P < 0.005$ , \*\*\* $P < 0.0005$  versus WT;  $^cP < 0.0005$  versus WT;  $^cP < 0.0005$  versus WT; CL, CL-316,243.

(1–4). Therefore, we next asked whether elevated  $\beta$ -AR expression by TET deficiency influenced adipocyte sensitivity to  $\beta$ -adrenergic stimuli. Treatment of WT and *Tet* TKO adipocytes with CL-316,243, a selective  $\beta$ -AR agonist, revealed that the intracellular  $\beta$ -adrenergic signaling was more potently activated in *Tet* TKO adipocytes compared to WT controls, as determined by higher levels of phosphorylated forms of PKA substrates and HSL in the stimulated *Tet* TKO adipocytes (Fig. 1E). Consistent with these results, *Tet* TKO significantly increased the rate of lipolysis stimulated by isoproterenol (ISO), a pan- $\beta$ -AR agonist, as assessed by the increased release of ISO-stimulated glycerol and free fatty acids in the *Tet* TKO adipocytes, when compared to WT controls (Fig. 1F and G). TET deficiency also significantly promoted lipolysis in adipocytes stimulated with forskolin or isobutylmethylxanthine (IBMX) that increased the concentration of intracellular cAMP (Fig. 1H), presumably due to the enhancement of pre-coupled stable complexes between the  $\beta$ -AR and adenylyl cyclase as a result of  $\beta$ -AR up-regulation (7). Furthermore, the oxygen consumption rate remained comparable between WT and *Tet* TKO adipocytes under basal conditions, but the CL-316,243-dependent oxygen consumption rate and proton leak were significantly increased in *Tet* TKO adipocytes, when compared to WT controls (Fig. 1I and J). TET deficiency also substantially enhanced fatty acid oxidation in ISO-stimulated adipocytes (Fig. 1K). Thus,

these results suggest that TET deficiency renders adipocytes more sensitive to  $\beta$ -AR signals by up-regulating  $\beta$ -AR expression.

We next determined whether TET deficiency elicited enhanced thermogenic gene expression by up-regulating  $\beta$ -AR expression. In agreement with a previous report (39), TET deficiency alone could significantly up-regulate a broad panel of thermogenesis-related genes (SI Appendix, Fig. S2A; control), confirming that TET proteins directly regulated their expression. Indeed, *Tet* TKO adipocytes possessed approximately fourfold higher *Pparg1a* promoter-driven reporter activity than did WT adipocytes (SI Appendix, Fig. S3A). TET proteins suppressed *Pparg1a* promoter activity through the CREB-binding element (CRE) that was previously shown to be responsive to  $\beta$ -AR signaling (SI Appendix, Fig. S3A and B) (44), and this suppression did not require their catalytic activities (SI Appendix, Fig. S3C). Instead, chromatin immunoprecipitation followed by qRT-PCR (ChIP-qPCR) showed that TET deficiency blocked the recruitment of HDAC1 to the *Pparg1a* and *Ucp1* gene loci, leading to an accumulation of acetylated H3K27, the active histone mark (SI Appendix, Fig. S3D and E). In both WT and *Tet* TKO adipocytes, forskolin considerably up-regulated *Pparg1a*, *Ucp1*, *Ppara*, *Elovl3*, and *Cidea*; however, this up-regulation was more robust in *Tet* TKO cells (SI Appendix, Fig. S2A). Neither *Tet* deficiency nor forskolin affected the expression of adipogenic *Pparg* and *Fabp4* marker

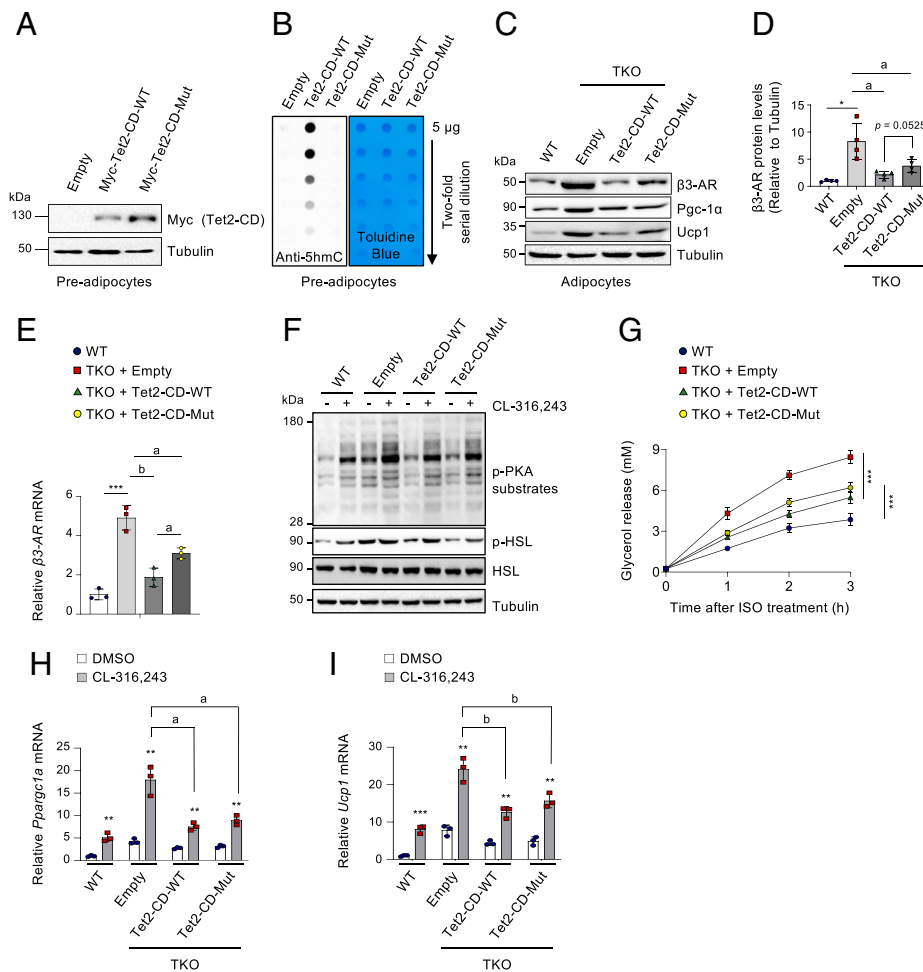


**Fig. 2.** TET proteins control  $\beta$ 3-AR expression and signaling in an enzymatic activity-independent manner. (A) Immunoblot analysis of Myc-tagged WT and mutant (Mut) Tet2 catalytic domain (Tet2-CD) in preadipocytes derived from iWAT of *Tet1<sup>fl/fl</sup> Tet2<sup>fl/fl</sup> Tet3<sup>fl/fl</sup> Cre-ERT2* mice.  $\alpha$ -Tubulin served as a loading control. *n* = 3. (B) Dot blot analysis to quantify genomic 5hmCs in cells shown in A. Toluidine blue staining confirmed blotting of equal amounts of DNA. *n* = 3. (C) Immunoblot analysis of  $\beta$ 3-AR, Pgc-1 $\alpha$ , and Ucp1 proteins in differentiated WT adipocytes or *Tet* TKO adipocytes expressing empty vector, WT, or mutant Tet2-CD.  $\alpha$ -Tubulin served as a loading control. *n* = 4. (D) Quantification of  $\beta$ 3-AR proteins presented in C. *n* = 4. (E) mRNA levels of  $\beta$ 3-AR relative to *Gapdh* in adipocytes shown in C. *n* = 3. (F) Immunoblot analysis of phosphorylated (p)-PKA substrates, p-HSL, and total HSL proteins in adipocytes shown in C after stimulation with or without CL-316,243 (10  $\mu$ M, 5 min).  $\alpha$ -Tubulin served as a loading control. (G) In vitro lipolysis in adipocytes shown in C. Plasma glycerol was quantified after stimulation with or without ISO (5  $\mu$ M) at the indicated time points. *n* = 6. (H and I) mRNA levels of *Pparg1a* (H) and *Ucp1* (I) relative to *Gapdh* in adipocytes shown in C after stimulation with or without CL-316,243 (1  $\mu$ M, 24 h). *n* = 3. All data are presented as the mean  $\pm$  SD. The *P* values were determined by unpaired Student's *t* test. \**P* < 0.05, \*\**P* < 0.005, \*\*\**P* < 0.0005 versus WT; <sup>a</sup>*P* < 0.05, <sup>b</sup>*P* < 0.005.

gene expressions (SI Appendix, Fig. S2B). Furthermore, acute stimulation with CL-316,243 also increased the mRNA levels of these thermogenic genes in WT adipocytes, and this was further enhanced in *Tet* TKO adipocytes (Fig. 1 L and M and SI Appendix, Fig. S3F; panels 1 and 2). Notably, pretreatment with SR59230A, a  $\beta$ 3-AR antagonist, substantially blocked the stimulatory effect of CL-316,243 in both WT and *Tet* TKO adipocytes (Fig. 1 L and M and SI Appendix, Fig. S3F; compare panels 2 and 4), confirming that  $\beta$ 3-AR up-regulation by TET deficiency was mainly responsible for the increased thermogenic gene expression during  $\beta$ -adrenergic stimulation.

**TET Proteins Suppress  $\beta$ 3-AR Expression and Signaling, Which Is Mainly Independent of Enzymatic Activity.** To further confirm whether the enzymatic activities of TET proteins were implicated in the control of thermogenic gene expression, the immortalized preadipocytes derived from iWAT of *Tet1<sup>fl/fl</sup> Tet2<sup>fl/fl</sup> Tet3<sup>fl/fl</sup> Cre-ERT2* mice were transduced with lentiviruses expressing WT or a catalytically inactive mutant version of the Myc-tagged Tet2 catalytic domain (Tet2-CD), which was previously shown to reverse loss of 5hmC and the effects by TET deficiency (45–47). Immunoblotting and dot blot assays validated appropriate Tet2 expression and activity (Fig. 2 A and B). As previously shown, both mRNA and protein levels of  $\beta$ 3-AR were up-regulated in differentiated adipocytes after induction of *Tet* deletion at day 2 of differentiation (Fig. 2 C–E). However, this up-regulation was substantially inhibited by ectopic expression of both WT and mutant Tet2-CD, although the catalytic mutant exhibited slightly weaker inhibitory

effects (Fig. 2 C–E). Consistently, both WT and mutant Tet2-CD similarly attenuated intracellular  $\beta$ -adrenergic signaling (Fig. 2F), lipolysis (Fig. 2G), and thermogenic gene induction (Fig. 2 H and I and SI Appendix, Fig. S4 A–C) in *Tet* TKO adipocytes upon  $\beta$ -agonist treatment. As expected, the Pgc-1 $\alpha$  and Ucp1 protein levels were also significantly down-regulated by Tet2-CD regardless of its enzymatic activity (Fig. 2C and SI Appendix, Fig. S4 D–F).

**Adipocyte-Specific TET Ablation Increases the Responsiveness to  $\beta$ 3-AR Signals In Vivo.**  $\beta$ 3-AR stimulation triggers beige adipocyte induction and activation in both murine and human ATs (6–8). To test whether elevated levels of  $\beta$ 3-AR in *Tet* TKO adipocytes affect fat browning under adrenergic stimulation, we generated adipose-specific *Tet* TKO mice by crossing *Tet1<sup>fl/fl</sup> Tet2<sup>fl/fl</sup> Tet3<sup>fl/fl</sup>* mice with *Adiponectin-Cre* mice (48). We deleted all three *Tet* genes to exclude potential functional compensation among TET family members that is commonly observed in various tissues (32, 49, 50). We verified successful *Tet* deletion and the resulting 5hmC diminution specifically in adipose tissues but not in the liver, kidney, pancreas, and other nonadipose tissues (SI Appendix, Fig. S5 A–C). Furthermore, *Tet* deletion was induced only in mature adipocytes within adipose depots and not in stromal vascular fraction cells containing preadipocytes and leukocytes (SI Appendix, Fig. S5 D and E).

To assess whether TET proteins influence  $\beta$ 3-AR agonist-triggered browning in vivo, WT and *Tet* TKO mice were administered CL-316,243 daily for three consecutive days, a condition

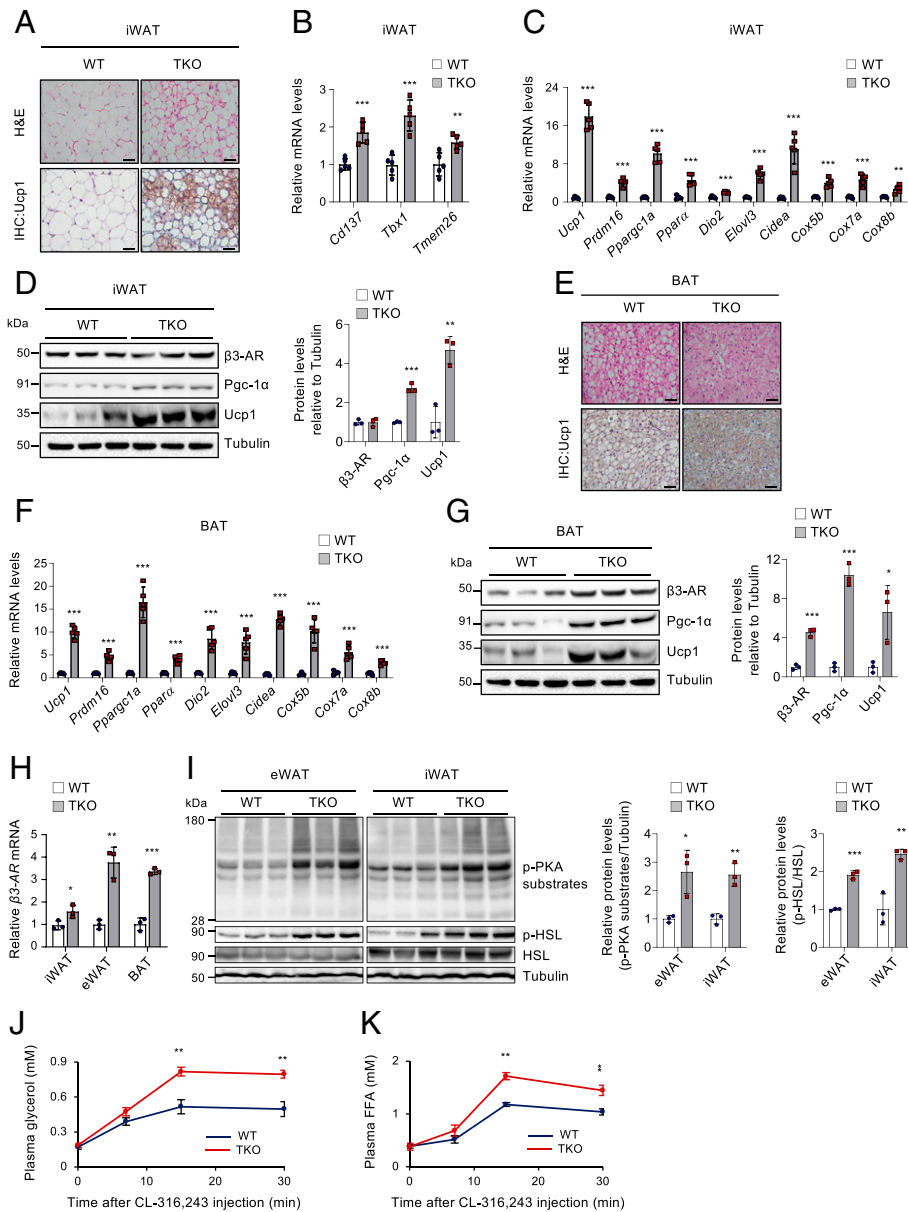


**Fig. 3.** Adipose TET deficiency increases the responsiveness to  $\beta$ 3-AR agonist in vivo. WT and *Tet* TKO mice were administered CL-316,243 (1 mg/kg body weight/d) intraperitoneally daily for three consecutive days. (A) Representative hematoxylin and eosin (H&E) (Top) and immunohistochemical staining for Ucp1 (Bottom) in iWAT of CL-316,243-treated mice.  $n = 4$ . (Scale bar, 50  $\mu$ m.) (B and C) mRNA levels of beige adipocyte-selective genes (B) or thermogenesis-related genes (C) relative to *Gapdh* in iWAT of CL-316,243-treated mice.  $n = 5$ . (D) Immunoblot analysis (Left) and quantification (Right) of  $\beta$ 3-AR, Pgc-1 $\alpha$ , and Ucp1 proteins in iWAT of CL-316,243-treated mice.  $\alpha$ -Tubulin served as a loading control.  $n = 3$ . (E) Representative H&E (Top) and immunohistochemical staining for Ucp1 (Bottom) in BAT of CL-316,243-treated mice.  $n = 4$ . (Scale bar, 50  $\mu$ m.) (F) mRNA levels of thermogenesis-related genes relative to *Gapdh* in BAT of CL-316,243-treated mice.  $n = 5$ . (G) Immunoblot analysis (Left) and quantification (Right) of  $\beta$ 3-AR, Pgc-1 $\alpha$ , and Ucp1 proteins in BAT of CL-316,243-treated mice.  $\alpha$ -Tubulin served as a loading control.  $n = 3$ . (H)  $\beta$ 3-AR mRNA levels relative to *Gapdh* in ATs (iWAT, eWAT, or BAT) of CL-316,243-treated mice.  $n = 3$ . (I) Immunoblot analysis (Left) and quantification (Right) of phosphorylated (p)-PKA substrates, p-HSL, and total HSL proteins in eWAT or iWAT of CL-316,243-treated mice.  $\alpha$ -Tubulin served as a loading control.  $n = 3$ . (J and K) In vivo lipolysis assay in WT and *Tet* TKO mice stimulated with CL-316,243. Plasma glycerol (J) and free fatty acid (FFA) (K) levels were quantified at the indicated time points.  $n = 3$ . All data are presented as the mean  $\pm$  SD. The  $P$  values were determined by unpaired Student's  $t$  test. \* $P < 0.05$ , \*\* $P < 0.005$ , \*\*\* $P < 0.0005$  versus WT. IHC, immunohistochemistry.

that induces mild fat browning (6). Histological analyses revealed that the iWAT of *Tet* TKO mice possessed more abundant Ucp1<sup>+</sup> multilocular adipocytes following CL-316,243 treatment compared to WT control (Fig. 3A). The iWAT of *Tet* TKO mice also displayed higher mRNA levels of genes associated with beiging (namely, *Cd137*, *Tbx1*, and *Tmem26*), thermogenesis (e.g., *Ucp1*, *Ppargc1a*, *Ppar $\alpha$* ), lipolysis (e.g., *Pnpl2*, *Lipe*), and fatty acid oxidation (e.g., *Acadm*, *Acadl*, *Acox1*) (Fig. 3B and C and SI Appendix, Fig. S6 A and B). Levels of Pgc-1 $\alpha$  and Ucp1 proteins were also higher in the iWAT of *Tet* TKO mice (Fig. 3D). A previous report showed that mice with *Fabp4-Cre*-mediated deletion of *Tet1* exhibited a depot-specific effect; they displayed increased thermogenic gene expression only in iWAT but not in BAT (39). However, the interscapular BAT of *Tet* TKO mice showed similar phenotypes as those observed in iWAT, including enhanced browning (Fig. 3E) and an elevated expression of  $\beta$ 3-AR and genes associated with thermogenesis, lipolysis, and fatty acid oxidation (Fig. 3F and G and SI Appendix, Fig. S6 C and D). Furthermore, both iWAT and BAT from *Tet* TKO mice contained higher amounts of mitochondrial DNAs compared to those from WT controls (SI Appendix, Fig. S6 E and F).

Together, these results suggest that TET loss promotes BAT activation as well as WAT browning. Notably, the mRNA levels of  $\beta$ 3-AR were higher in adipose depots (i.e., iWAT, eWAT, and BAT) from *Tet* TKO mice, more prominently in the latter two, when compared to WT controls (Fig. 3H). Consistently, *Tet* TKO mice displayed enhanced  $\beta$ -adrenergic signaling and in vivo lipolytic responses upon  $\beta$ 3-AR agonist treatment, as determined by increased phosphorylation of PKA substrates and HSL (Fig. 3I), and more robust release of plasma glycerol and free fatty acids (Fig. 3J and K). Collectively, these results suggest that adipose TET deficiency leads to elevated  $\beta$ 3-AR expression and increases the sensitivity to  $\beta$ 3-AR stimulation in vivo.

**Adipocyte-Specific *Tet* TKO Mice Are Resistant to Diet-Induced Obesity.**  $\beta$ 3-AR is substantially repressed in various animal models of obesity, and this  $\beta$ 3-AR down-regulation has been considered a key contributing factor that causes catecholamine resistance in obesity (16–18). As TET proteins negatively regulated  $\beta$ 3-AR, we next asked whether *Tet* expression was altered under persistent nutrient surplus. Notably, levels of *Tet1*, *Tet2*, and *Tet3* mRNAs (Fig. 4A) and those of 5hmCs (Fig. 4B and C) were significantly

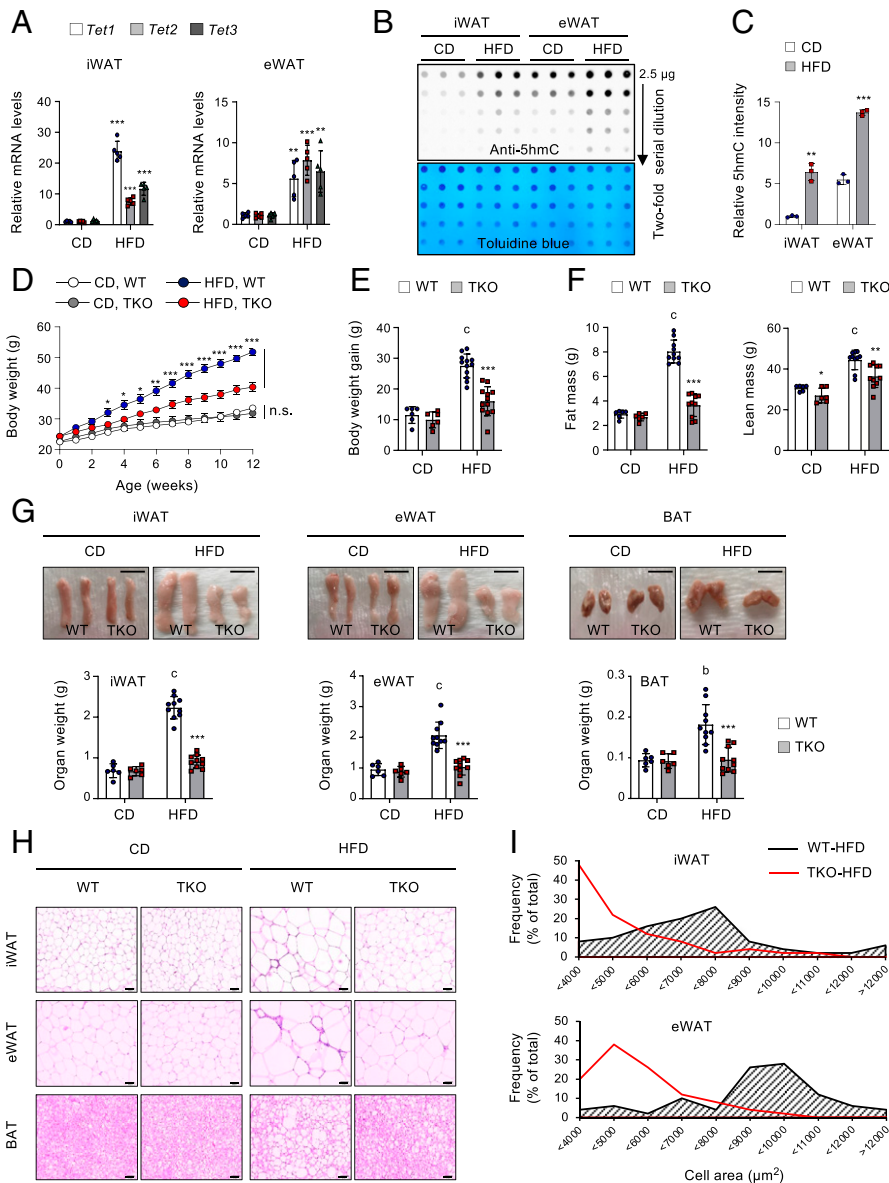


**Fig. 4.** Adipocyte *Tet* expression is elevated in obesity, and *Tet* TKO mice resist diet-induced obesity. (A) *Tet1*, *Tet2*, and *Tet3* mRNA levels relative to *Gapdh* in iWAT and eWAT from C57BL/6 male mice fed either CD or HFD for 12 wk. *n* = 5. (B) Genomic 5hmC levels in iWAT and eWAT from the mice shown in A. Toluidine blue staining confirmed blotting of equal amounts of DNAs. (C) Quantification of relative 5hmC intensity from the image shown in B. (D) Changes in body weight of WT and *Tet* TKO mice fed either CD or HFD. *n* = 6–12. (E) Summary of body weight gain in WT and *Tet* TKO mice fed either CD (*n* = 6) or HFD (*n* = 12) for 12 wk. (F) Absolute amount of fat mass (Left) and lean mass (Right) from WT and *Tet* TKO mice fed either CD (*n* = 6) or HFD (*n* = 10). (G) Representative photographs of iWAT, eWAT, and BAT of WT and *Tet* TKO mice fed either CD or HFD (Top). A summary of the weights of each fat pad is also shown (Bottom). *n* = 6 mice fed CD; *n* = 10 mice fed HFD. (Scale bar, 1 cm.) (H and I) Hematoxylin and eosin staining (H; *n* = 10) and frequency distribution of adipocyte cell size (I) in iWAT and eWAT of WT and *Tet* TKO mice fed either CD or HFD. (Scale bar, 100  $\mu$ m.) All data are presented as the mean  $\pm$  SD. The *P* values were determined by unpaired Student's *t* test. \**P* < 0.05, \*\**P* < 0.005, \*\*\**P* < 0.0005 versus WT; <sup>b</sup>*P* < 0.005, <sup>c</sup>*P* < 0.0005 versus CD. n.s., not significant.

elevated in iWAT and epididymal WAT (eWAT) of mice fed a HFD (60% energy as fat) compared to the levels in mice fed a chow diet (CD; 10% energy as fat). *TET1*, *TET2*, and *TET3* mRNA levels also tended to increase in patients with obesity or diabetes, compared to lean individuals, although this difference did not reach statistical significance, possibly due to negative feedback on TET expression in humans under obese or diabetic conditions (SI Appendix, Fig. S7A). These results suggest that *Tet* expression and function are nutritionally regulated in ATs and that TET proteins may play a role in diet-induced obesity.

To clarify the physiological function of TET proteins in the development of obesity, *Tet* TKO and WT littermate mice were fed either a CD or HFD for 12 wk, starting at 8 wk of age. There was no difference in weight gain in response to the CD (Fig. 4D and E and SI Appendix, Fig. S7B). However, *Tet* TKO mice were more resistant to weight gain in response to a HFD than were WT mice, despite comparable food intakes (Fig. 4D and E and SI Appendix, Fig. S7B and C). The lower body weight of *Tet* TKO mice primarily resulted from a reduction in fat mass with only a marginal alteration in lean body mass (Fig. 4F and SI Appendix, Fig. S7D and E). Examination of dissected fat tissues confirmed that iWAT, eWAT, and BAT

were significantly smaller in these mice (Fig. 4G). Histologically, both WAT and BAT from HFD-fed *Tet* TKO mice contained adipocytes possessing smaller lipid droplets compared with those of WT controls, whereas there was no discernible difference in adipocyte size of mice fed a CD (Fig. 4H and I). Upon HFD feeding, the average adipocyte size increased by  $\sim 3.56$ -fold in iWAT of WT mice but only  $\sim 1.68$ -fold in *Tet* TKO mice, and similar reductions were also observed in eWAT (by  $\sim 1.41$ -fold) and BAT (by  $\sim 3.25$ -fold) of *Tet* TKO mice (SI Appendix, Fig. S7F). These data indicate that adipose TET deficiency robustly inhibits the development of obesity and obesity-induced adipocyte hypertrophy. Previous reports suggested that TET proteins were required for early adipogenic differentiation in vitro (40, 41). However, the observed difference in body weight change was not attributable to impaired adipogenesis in vivo because mRNA levels of known markers or regulators of adipogenesis were comparable between WT and *Tet* TKO mice on either diet, consistent with the fact that adiponectin-Cre we used was active in mature adipocytes (48) (SI Appendix, Fig. S7G–J). Furthermore, we confirmed that *Tet* TKO female mice were also resistant to diet-induced obesity, mainly due to a reduction in fat mass (SI Appendix, Fig. S8).

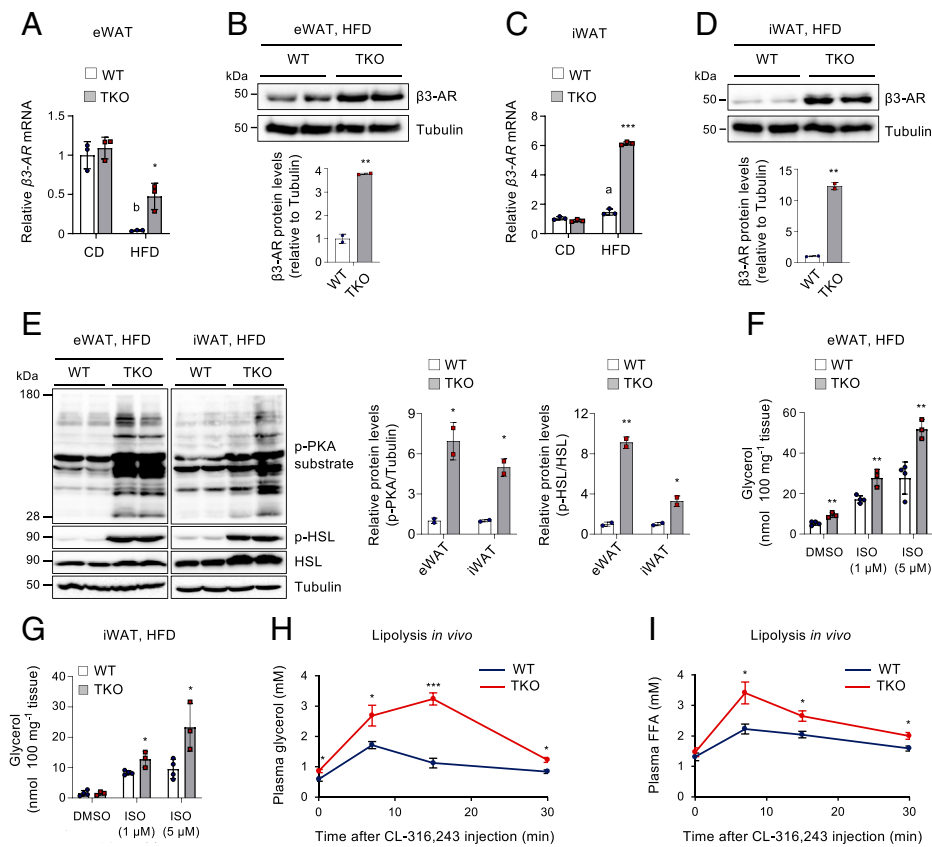


**Fig. 5.** TET deficiency resists obesity-associated catecholamine resistance by blocking  $\beta_3$ -AR reduction during diet-induced obesity. (A)  $\beta_3$ -AR mRNA levels relative to *Gapdh* in eWAT from WT and *Tet* TKO mice fed either CD or HFD.  $n = 3$ . (B) Immunoblot analysis (Top) and quantification (Bottom) of  $\beta_3$ -AR proteins in eWAT from WT and *Tet* TKO mice fed an HFD.  $\alpha$ -Tubulin served as a loading control. (C)  $\beta_3$ -AR mRNA levels relative to *Gapdh* in iWAT from WT and *Tet* TKO mice fed either CD or HFD.  $n = 3$ . (D) Immunoblot analysis (Top) and quantification (Bottom) of  $\beta_3$ -AR proteins in iWAT from WT and *Tet* TKO mice fed an HFD.  $\alpha$ -Tubulin served as a loading control. (E) Immunoblot analysis (Left) and quantification (Right) of phosphorylated (p)-PKA substrates, p-HSL, and total HSL proteins in eWAT or iWAT from HFD-fed WT and *Tet* TKO mice.  $\alpha$ -Tubulin served as a loading control. (F and G) Ex vivo lipolysis in eWAT (F) and iWAT (G) isolated from HFD-fed WT and *Tet* TKO mice after stimulation with or without ISO at the indicated concentrations.  $n = 3$ –4. (H and I) In vivo lipolysis in HFD-fed WT and *Tet* TKO mice. Plasma glycerol (H) and free fatty acid (I) levels were quantified after administration of CL-316,243.  $n = 3$ –4. All data are presented as the mean  $\pm$  SD. The  $P$  values were determined by unpaired Student's  $t$  test. \* $P < 0.05$ , \*\* $P < 0.005$ , \*\*\* $P < 0.0005$  versus WT; <sup>a</sup> $P < 0.05$ , <sup>b</sup> $P < 0.005$  versus CD. DMSO, dimethyl sulfoxide.

**Adipocyte-Specific *Tet* TKO Mice Resist  $\beta_3$ -AR Reduction and Catecholamine Resistance during Diet-Induced Obesity.** Activation of the  $\beta_3$ -adrenergic signaling increases energy expenditure by triggering lipolysis, fatty acid oxidation, and thermogenesis, ultimately leading to a decline in fat accumulation and obesity resistance (1, 2). Thus, we next sought to determine whether the restricted AT hypertrophy in the HFD-fed *Tet* TKO mice resulted from increased  $\beta$ -adrenergic responsiveness through enhanced  $\beta_3$ -AR expression.  $\beta_3$ -AR was substantially suppressed in eWAT of WT mice after 12 wk on a HFD, but this was substantially blocked in *Tet* TKO mice (Fig. 5A). Protein levels of  $\beta_3$ -AR also remained significantly higher in HFD-fed *Tet* TKO mice (Fig. 5B). HFD feeding did not affect  $\beta_3$ -AR mRNA levels in iWAT and BAT of WT mice, but TET deficiency led to an elevated  $\beta_3$ -AR expression in these ATs following HFD feeding (Fig. 5C and D and *SI Appendix*, Fig. S9A). Consistent with the higher levels of  $\beta_3$ -AR expression, both eWAT and iWAT of HFD-fed *Tet* TKO mice displayed significantly enhanced  $\beta$ -AR signaling, as determined by increased phosphorylation of PKA substrates and HSL (Fig. 5E).

To further confirm whether increased  $\beta_3$ -AR expression and signaling affect lipolytic responses, eWAT and iWAT were isolated from HFD-fed WT or *Tet* TKO mice and treated with ISO. The ISO-stimulated lipolysis, as assessed by the release of glycerol and free fatty acids, was significantly enhanced in these explants of *Tet* TKO mice compared to those from WT mice (Fig. 5F and G and *SI Appendix*, Fig. S9B). Moreover, TET deficiency also significantly promoted lipolysis in isolated primary ATs treated with forskolin or IBMX (*SI Appendix*, Fig. S9C). We also observed a mild increase in lipolytic responses in the BAT from *Tet* TKO mice (*SI Appendix*, Fig. S9D and E). To further confirm the lipolytic activity in vivo, we injected mice intraperitoneally with CL-316,243. Consistent with data obtained in vitro, the serum glycerol and free fatty acid levels

were significantly higher in *Tet* TKO mice than in WT mice (Fig. 5H and I). Together, these results suggest that TET deficiency resisted  $\beta_3$ -AR reduction during chronic HFD challenges and thereby rendered adipocytes more sensitive to catecholamines. This may have contributed to the maintenance of higher levels of  $\beta$ -agonist-stimulated lipolytic capacity and resistance to adipocyte hypertrophy.

**Adipose TET Deficiency Leads to the Maintenance of Higher Capacity for Thermogenesis and Energy Expenditure during Chronic Overnutrition.** Excess caloric intake activates thermogenesis as a means to increase energy expenditure to prevent excess fat accumulation and obesity (3, 4). This diet-induced thermogenesis is critically dependent on  $\beta$ -AR signaling (3, 4). However, energy expenditure fails to fully compensate for chronic overnutrition during the development of obesity. Indeed, consistent with  $\beta$ -AR reduction and decreased  $\beta$ -AR responses, obese humans and animals display diminished adipose thermogenesis (51). As  $\beta_3$ -AR expression and  $\beta$ -adrenergic responsiveness were maintained at higher levels in *Tet* TKO mice fed an HFD, we next examined whether TET deficiency resists the reduction of energy expenditure and thermogenesis during chronic overnutrition. To test this possibility, we first performed indirect calorimetry on HFD-fed WT and *Tet* TKO mice maintained at different ambient temperatures (30 °C, 22 °C, and 4 °C). HFD-fed *Tet* TKO mice exhibited significantly higher rates of oxygen consumption ( $V_{O_2}$ ), carbon dioxide production ( $V_{CO_2}$ ), and heat dissipation under all conditions, and these alterations became more pronounced as the temperature dropped (Fig. 6A–D and *SI Appendix*, Fig. S10A and B). However, the levels of motor activity were comparable between both groups of mice (*SI Appendix*, Fig. S10C). The respiratory exchange rate ( $V_{CO_2}/V_{O_2}$ ) indicated that a greater proportion of carbohydrate metabolism was preserved in HFD-fed *Tet* TKO mice during dark periods at 22 °C

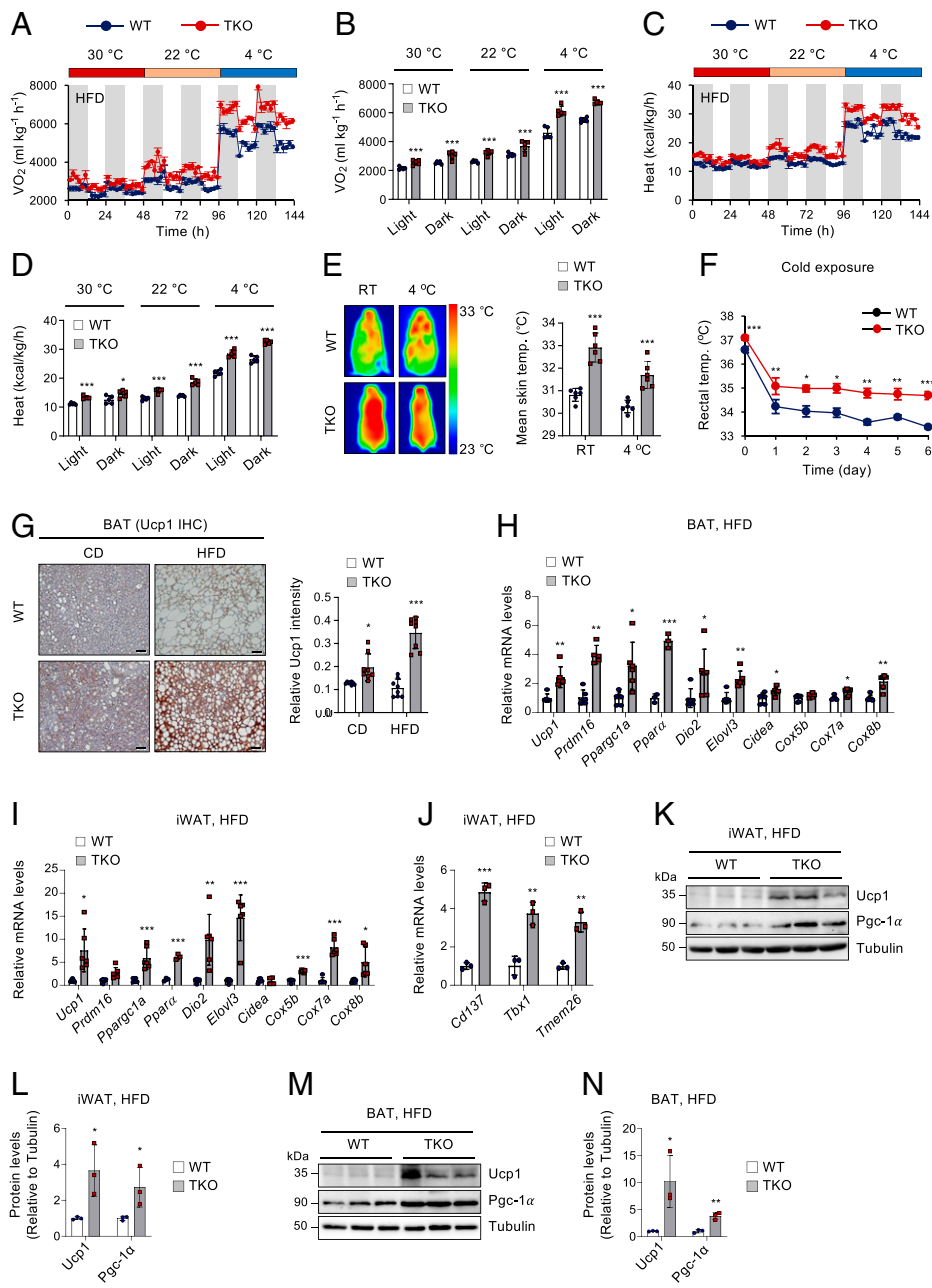


**Fig. 6.** TET deficiency leads to the maintenance of a higher capacity for thermogenesis and energy expenditure under chronic overnutrition. (A–D) Indirect calorimetry of HFD-fed WT and *Tet* TKO mice maintained at 30°C, 22°C, and 4°C to obtain  $VO_2$  (A), average  $VO_2$  (B), heat production (C), and average heat production (D) data.  $n = 5$ . (E) Representative dorsal infrared thermal images (Left) and mean skin temperature (Right) of HFD-fed WT and *Tet* TKO mice housed at room temperature (RT) or 4°C for 1 wk.  $n = 6$ . (F) Changes in rectal temperatures of HFD-fed WT and *Tet* TKO mice during cold exposure.  $n = 7$  WT mice;  $n = 9$  *Tet* TKO mice. (G) Representative immunohistochemical staining for Ucp1 ( $n = 6$ ; Left) in BAT sections from WT and *Tet* TKO mice fed either CD or HFD for 12 wk. Quantification results are also shown (Right).  $n = 8$ . (Scale bar, 100  $\mu$ m.) (H and I) mRNA levels of thermogenesis-related genes relative to *Gapdh* in BAT (H) or iWAT (I) from HFD-fed WT and *Tet* TKO mice.  $n = 5$ –6 (except *Ppara $\alpha$* ,  $n = 3$ ). (J) mRNA levels of beige adipocyte-selective genes relative to *Gapdh* in iWAT from HFD-fed WT and *Tet* TKO mice.  $n = 3$ . (K–N) Immunoblot analysis and quantification of Ucp1 and Pgc-1 $\alpha$  proteins in iWAT (K and L) or BAT (M and N) from WT and *Tet* TKO mice.  $n = 3$ . ( $\alpha$ -Tubulin served as a loading control.  $n = 3$ . All data are presented as the mean  $\pm$  SD. The *P* values were determined by unpaired Student's *t* test. \* $P < 0.05$ , \*\* $P < 0.005$ , \*\*\* $P < 0.0005$  versus WT. IHC, immunohistochemistry.

and 4°C (SI Appendix, Fig. S10D), which was likely due to reduced fat deposition. To further correct metabolic rates for body mass, we performed regression-based ANCOVA using body weights as a covariate. We observed a group-specific effect between WT and *Tet* TKO mice, which was independent of a difference in body mass at 30°C and 4°C, whereas both genotypes fell on a similar regression line at 22°C (SI Appendix, Fig. S10E). It is possible that the effect was stronger at 4°C because levels of catecholamine released by sympathetic nerve terminals were up-regulated upon cold exposure. As *Tet*-deficient adipocytes express higher  $\beta_3$ -AR compared to WT cells, they would exhibit stronger responsiveness to the catecholamines. When we plotted ANCOVA-predicted metabolic rates at a given body mass of 40 g (kcal/h/40 g), as suggested previously as an alternative analysis when there is absolutely no overlap in the data from two groups on the mass axis (52, 53), as observed in our cases (Fig. 4), *Tet* TKO mice displayed significantly higher metabolic rates compared to WT mice under all conditions (SI Appendix, Fig. S10F).

Together, these results indicate that *Tet* TKO mice maintained a higher capacity of thermogenesis despite chronic overnutrition. Consistent with these observations, HFD-fed *Tet* TKO mice maintained significantly higher surface and core (rectal) temperatures than did WT littermates under basal conditions and after cold exposure (Fig. 6 E and F and SI Appendix, Fig. S10G). Thus, these results suggest that TET proteins restrict adaptive thermogenesis and energy expenditure during periods of chronic overnutrition.

Consistent with these observations, HFD-fed *Tet* TKO mice possessed smaller brown adipocytes with increased Ucp1 expression in BAT compared to WT controls (Fig. 6G) and exhibited elevated levels of thermogenic genes in both BAT and iWAT (Fig. 6 H and I). They also showed higher mRNA expressions of beiging marker genes in iWAT (Fig. 6J). The levels of Ucp1 and Pgc-1 $\alpha$  proteins were also significantly higher in both iWAT and BAT of HFD-fed TKO mice (Fig. 6 K–N). Furthermore, HFD consumption significantly reduced the expression of *Ppargc1a*, a



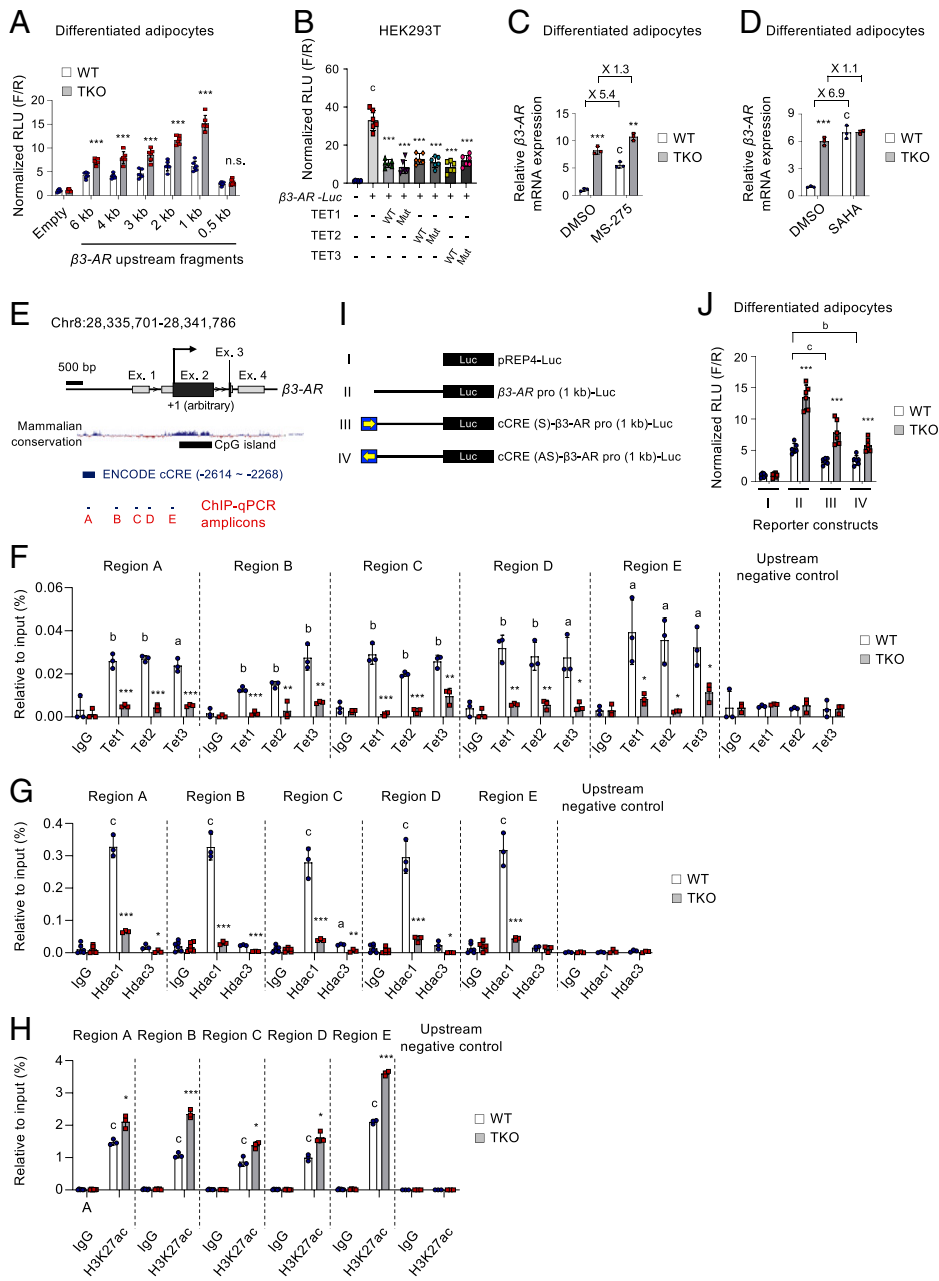


**Fig. 7.** TET proteins cooperate with HDACs to directly suppress  $\beta 3$ -AR transcription. (A) pREP4-based luciferase reporter activities driven by serially truncated  $\beta 3$ -AR promoters in WT and *Tet* TKO adipocytes. Results were normalized to Renilla luciferase activity.  $n = 6$ . (B) pREP4-based luciferase reporter activities driven by the  $\beta 3$ -AR (1 kb) promoter in HEK293T cells transfected with WT or mutant TET1, TET2, and TET3 plasmids.  $n = 6$ . (C and D) mRNA expression of  $\beta 3$ -AR relative to *Gapdh* in WT and *Tet* TKO adipocytes stimulated with or without MS-275 (10  $\mu$ M, 24 h) (C) or a pan-HDAC inhibitor, SAHA (20  $\mu$ M, 6 h) (D).  $n = 3$ . (E) The genomic configuration of the mouse  $\beta 3$ -AR gene locus. Locations of ChIP-qPCR amplicons, mammalian conservation, CpG islands, and Encyclopedia of DNA Elements (ENCODE) *cis*-CRE (cCRE) are shown. (F–H) ChIP-qPCR assays for Tet1, Tet2, and Tet3 (F); HDAC1 and HDAC3 (G); and acetylated H3K27 (H3K27ac) (H) for regions A–E shown in E. Enrichment at the nonbinding  $\beta 3$ -AR upstream region was used as a negative control.  $n = 3$ . (I) Schematic representation of the  $\beta 3$ -AR (1 kb) promoter-driven luciferase constructs. Yellow arrows indicate the direction of the incorporated ENCODE cCRE element shown in E. (J) pREP4-based luciferase reporter assay for the  $\beta 3$ -AR promoters shown in (I) in WT and *Tet* TKO adipocytes.  $n = 6$ . All data are presented as the mean  $\pm$  SD. The  $P$  values were determined by unpaired Student's  $t$  test. \* $P < 0.05$ , \*\* $P < 0.005$ , \*\*\* $P < 0.0005$  versus WT; <sup>a</sup> $P < 0.05$ , <sup>b</sup> $P < 0.005$ , <sup>c</sup> $P < 0.0005$  versus reporter only (B), dimethyl sulfoxide (DMSO) (C), immunoglobulin G (IgG) (F–H), and reporter II in WT (J). Ex, exon; Mut, catalytically inactive mutant; n.s., not significant; RLU, relative light units; F/R, firefly/renilla.

critical regulator of mitochondrial biogenesis and energy metabolism (54), in iWAT and eWAT, which was potentially blocked by TET deficiency (SI Appendix, Fig. S11A). *Ppargc1a* was also maintained at a higher level in BAT from HFD-fed *Tet* TKO mice. Consistently, various adipose depots from HFD-fed *Tet* TKO mice maintained higher mitochondrial DNA content and fatty acid oxidation capacity (SI Appendix, Fig. S11 B and C). Together, these data suggest that elevated TET expression in chronic overnutrition may promote obesity by limiting the energy expenditure and thermogenic potentials of both beige and BAT adipocytes.

**TET Proteins Cooperate with HDACs to Directly Repress  $\beta 3$ -AR Transcription in Adipocytes.** Given the inverse correlation between  $\beta 3$ -AR and *Tet* expressions, we assessed whether TET proteins could directly regulate  $\beta 3$ -AR promoter activity. We cloned serially truncated versions of the promoter regions (from 0.5 kb to 6 kb) of the mouse  $\beta 3$ -AR gene linked to a luciferase reporter ( $\beta 3$ -AR-Luc) into pREP4 plasmid that forms chromatin in mammalian cells (55, 56). Except for the 0.5-kb proximal

region, all fragments larger than 1 kb significantly stimulated reporter activities in WT adipocytes, and this was further enhanced in *Tet* TKO cells (Fig. 7A), indicating TET-mediated suppression of the  $\beta 3$ -AR promoter activity. In another reporter assay in HEK293T cells, both WT and catalytically inactive mutants of TET proteins were capable of suppressing the  $\beta 3$ -AR promoter activity, confirming that TET proteins controlled  $\beta 3$ -AR transcription, mainly in a catalytic activity-independent manner (Fig. 7B).

TET proteins often mediate transcriptional silencing through their incorporation into HDAC complexes (37–39). Thus, we next investigated whether HDACs are implicated in TET-mediated thermogenic gene regulation. MS-275, a selective inhibitor of HDAC1 and HDAC3, up-regulated various thermogenic genes in both WT and *Tet* TKO adipocytes; however, the fold induction by MS-275 was significantly decreased in *Tet* TKO cells compared to WT cells (Fig. 7C and SI Appendix, Fig. S12 A–C), suggesting the possible implication of HDACs, including HDAC1 and HDAC3, in TET-mediated  $\beta 3$ -AR suppression. However, upon MS-275 treatment, *Tet* TKO adipocytes

still expressed higher levels of thermogenic genes compared to WT controls. Thus, it is possible that additional HDACs other than class I HDACs may also be implicated in the TET-mediated suppression of these thermogenic genes. To test this possibility, we treated WT and *Tet* TKO adipocytes with suberoylanilide hydroxamic acid (SAHA; also known as vorinostat), a pan-HDAC inhibitor that potently inhibits class I and class II HDACs. SAHA exhibited little effects on thermogenic gene expression in *Tet* TKO adipocytes, whereas it robustly up-regulated it in WT controls (Fig. 7D and *SI Appendix*, Fig. S12 A and B). Furthermore, when treated with SAHA, both WT and *Tet* TKO adipocytes expressed thermogenic genes at comparable levels. Together, these results indicate that TET proteins directly repress  $\beta$ 3-AR and other thermogenic genes by modulating HDACs.

As previously reported (38, 39), we also confirmed that TET proteins physically associated with HDAC1 and HDAC3 (*SI Appendix*, Fig. S12 D–F). HDAC enzymes deacetylate histones and suppress transcription. ChIP-qPCR revealed that WT adipocytes exhibited a significant accumulation of all three TET proteins and HDAC1 on the upstream regulatory regions of the  $\beta$ 3-AR gene locus (Fig. 7 E–G). However, the occupancy of HDAC3 was very low and not significant when compared with enrichment by immunoglobulin G controls (Fig. 7G). Notably, *Tet* TKO adipocytes exhibited a diminished occupancy of both TET and HDAC1 proteins in the  $\beta$ 3-AR gene locus and thus possessed increased levels of acetylated H3K27, the active histone marker (Fig. 7 F–H). The immunoprecipitated genomic DNA samples showed no enrichment at the nonbinding region upstream of  $\beta$ 3-AR. These results suggest that TET proteins recruit HDAC1 to the  $\beta$ 3-AR gene promoter, ultimately leading to histone deacetylation for transcriptional suppression.

The Encyclopedia of DNA Elements project (57) predicted a 346-bp upstream DNA element located between  $-2,614$  and  $-2,268$  as one of the candidate *cis*-regulatory elements in the  $\beta$ 3-AR locus (Fig. 7E, *region A* and *SI Appendix*, Fig. S12G). This region is well conserved among mammalian species (Fig. 7E), and its histone acetylation was controlled by TET-HDAC interaction (Fig. 7 F–H, *region A*). To confirm the functionality of this element, we constructed additional reporters by incorporating this element upstream of the  $\beta$ 3-AR promoter (1 kb) in both orientations (Fig. 7I). The presence of this element significantly diminished  $\beta$ 3-AR promoter activity in adipocytes regardless of its orientation (Fig. 7J, *compare reporter activities in WT cells*), and this was significantly relieved by TET deficiency (Fig. 7J), confirming its silencer-like function. Together, these results indicate that TET proteins directly repress  $\beta$ 3-AR transcription by the epigenetic modification of its promoter via the recruitment of HDACs.

## Discussion

Here, we report that TET proteins are crucial epigenetic suppressors of  $\beta$ 3-AR expression and  $\beta$ -adrenergic responsiveness in adipocytes. A pan-TET deficiency significantly elevated  $\beta$ 3-AR expression and sensitivity to  $\beta$ -AR agonists in cultured cells and mice, thus potentiating the  $\beta$ 3-AR-triggered downstream responses, including lipolysis, thermogenic gene induction, mitochondrial respiration, and fat browning. Notably, adipose *Tet* expression was elevated by excess nutrient uptake. During the development of HFD-induced obesity, adipose-specific pan-TET deficiency led to the maintenance of higher  $\beta$ 3-AR expression and  $\beta$ -adrenergic responsiveness in both WAT and BAT. As a result, *Tet* TKO mice were strikingly resistant to diet-induced obesity, inflammation, and related metabolic defects.

Previous studies proposed the potential regulatory roles of TET proteins in adipocyte differentiation and function. However, knockdown of *Tet1* or *Tet2* exerts controversial effects on adipogenic differentiation in vitro (40–42). Our data show that TET proteins differentially affect adipogenesis in vitro, depending on the differentiation stage. Ablation of all TET proteins in preadipocytes or during adipogenic induction completely blocked the formation of mature adipocytes, but its loss at a later stage did not exhibit any significant antiadipogenic effects. TET proteins may be essential for the early adipogenic commitment of progenitor cells, presumably by regulating key adipogenic regulators, including PPAR $\gamma$ , as previously suggested (41, 58). However, they may be largely dispensable for adipogenesis after preadipocytes are committed to adipogenic lineage. Furthermore, a previous report showed that *Tet1* deletion in mice suppressed thermogenesis by repressing *Ucp1* and *Ppargc1a* in beige adipocytes (39). Thus, the *Tet1* knockout mice were partially protected from cold stress, diet-induced obesity, and associated metabolic dysfunctions. In contrast, another report showed that *Tet1* haploinsufficiency predisposed mice to diet-induced obesity and aggravated glucose intolerance (42). Thus, the exact roles of TET proteins in metabolism remain unclear. Here, we deleted all three *Tet* genes using *Adiponectin-Cre*, which is expressed in a highly adipocyte-specific manner (48, 59), and confirmed that triple TET deficiency substantially increases  $\beta$ 3-AR expression and function in both ATs and cultured adipocytes, and enhances fat lipolysis, browning, and thermogenic gene expression. The resulting phenotype was more pronounced than that of cells and mice rendered *Tet1*-deficient with *Fabp4-Cre* (39), which is expressed in both AT and nonadipose tissue (59). Furthermore, although *Tet1* deficiency was previously shown to increase thermogenic gene expression only in iWAT but not in BAT (39), our *Tet* TKO mice showed similar phenotypes in both WAT and BAT. The weaker phenotypes in *Tet1* knockout mice, compared to our *Tet* TKO mice, may be attributed to the functional redundancy among TET family members.

Our analysis identified  $\beta$ 3-AR as the direct target of TET proteins that, in turn, controlled downstream  $\beta$ -adrenergic responses. From a molecular standpoint, we showed that TET proteins recruited HDACs, particularly HDAC1, to the  $\beta$ 3-AR promoter to directly suppress its transcription. TET deficiency led to a dissociation of HDACs from the  $\beta$ 3-AR gene promoter, thereby switching the repressive chromatin state to the active state. Pharmacological inactivation of HDACs led to significant induction of various thermogenic genes in WT adipocytes, but its effect was decreased in *Tet* TKO adipocytes. Notably, this TET-HDAC cooperation occurred via a physical interaction between TET and HDAC enzymes, and functional cooperation did not require the catalytic activity of the TET proteins in reporter assays for  $\beta$ 3-AR promoter activities. HDACs, particularly class I HDACs, have recently emerged as promising molecular targets for treating obesity and type 2 diabetes (60). TET deficiency mimics the effects of HDAC inhibition in vitro and in vivo. Genetic or pharmacological inactivation of HDACs (particularly HDAC1 or HDAC3) simultaneously activates  $\beta$ 3-AR, *Ucp1*, and *Ppargc1a* by increasing histone acetylation at these gene loci (61–63). Consistently, HDAC inactivation in mice facilitates systemic energy expenditure by promoting WAT browning, lipolysis, thermogenesis, and oxidative metabolism, and thus prevents obesity and insulin resistance (61, 62, 64). All these phenotypes are recapitulated in our *Tet* TKO mice. Thus, TET proteins may control thermogenesis and energy expenditure by modulating the genomic distribution of HDACs. As TET deficiency resists the suppressive effects of chronic overnutrition on

$\beta$ 3-AR expression and function, targeting the TET-HDAC- $\beta$ 3-AR axis could provide a way to reprogram fat cell fates and functions to treat obesity and related metabolic diseases.

Our data also suggested that HFD-induced elevation of TET expression is causally linked to the initiation and development of diet-induced obesity.  $\beta$ 3-AR expression and  $\beta$ -adrenergic signaling are significantly suppressed during chronic nutrient overload, ultimately leading to catecholamine resistance in obesity (13–18). Despite chronic overnutrition, TET deficiency may allow for sustained catecholamine sensitivity by blocking  $\beta$ 3-AR down-regulation, thus enhancing  $\beta$ -adrenergic signaling, lipolysis, mitochondrial biogenesis, fatty acid oxidation, and thermogenesis. Ultimately, it may result in an overall increase in energy expenditure to prevent fat accumulation and obesity. Moreover, TET proteins seem to exert their primary effects at the level of lipolysis. TET loss leads to a remarkable increase in  $\beta$ -agonist-stimulated lipolysis *in vitro* and *in vivo*. The increased lipolysis may contribute to the maintenance of smaller and metabolically healthier adipocytes by robustly antagonizing fat storage and AT hypertrophy, despite excess nutrient uptake. AT expansion during periods of nutritional affluence promotes inflammation and adipocyte dysfunction (65). Consistent with reduced fat cell size, *Tet* TKO mice were markedly protected from inflammation and metabolic defects when fed an HFD (*SI Appendix*, Figs. S13–S15). Thus, it is likely that the improved metabolic phenotypes observed in the HFD-fed *Tet* TKO mice may primarily be attributable to the reduced AT hypertrophy and body weight gain. However, given the role of  $\beta$ 3-AR signals in antagonizing ectopic fat accumulation and obesity, our data suggest that TET-mediated modulation of catecholamine sensitivity may exert more fundamental effects on the metabolic phenotypes.  $\beta$ 3-ARs are abundantly expressed in murine ATs and serve as primary  $\beta$ -ARs. Agonists of  $\beta$ 3-ARs display antiobesity and antidiabetic effects in mice. However, low levels of  $\beta$ 3-AR expression in human white adipocytes (2, 66) seemed to limit the therapeutic efficacy of  $\beta$ 3-AR agonists in clinical trials (27). Thus, combined administration of selective  $\beta$ 3-AR agonists while boosting  $\beta$ 3-AR expression with pan-TET inhibitors may offer a therapeutic opportunity for treating human obesity and metabolic diseases.

It remains unknown how TET expression is up-regulated in ATs following HFD consumption. Recent studies have suggested that TET expression or function can be controlled by obesity- or type 2 diabetes-associated hyperglycemia (67–69). However, it was variably altered depending on the context and not directly assessed in ATs. In this regard, we note that 5hmC paradoxically accumulates more effectively under hypoxia (70–72), despite limited levels of oxygen, an essential cofactor for TET enzymes (32). HIF-1 $\alpha$  has been shown to activate *TET1*, *TET2*, and *TET3* transcription by directly binding to their promoters in various cells, including adipocytes

(70–72). As HFD-induced adipocyte expansion restricts oxygen availability within ATs (73), the subsequent HIF-1 $\alpha$  accumulation may stimulate *Tet* expression. Furthermore, recent studies showed that hypoxia-induced HIF-1 $\alpha$  triggers obesity-induced AT inflammation and adipocyte dysfunction, leading to insulin resistance (73). Notably, upon HFD feeding, mice lacking HIF-1 $\alpha$  in adipocytes largely phenocopied our *Tet* TKO mice, as both animal models exhibited resistance to diet-induced obesity, reduced macrophage accrual and inflammation, improved insulin sensitivity, glucose tolerance, and elevated energy expenditure and fatty acid oxidation (73–75). Together, these results suggest that adipose HIF-1 $\alpha$  and TET proteins may work in the same pathway to promote fat deposition and obesity in times of excessive nutrient uptake. More studies are warranted to determine whether and how the hypoxia–HIF-1 $\alpha$ –TET axis works to induce obesity and metabolic defects.

In summary, we identified TET proteins as pivotal epigenetic suppressors of  $\beta$ 3-AR in adipocytes that reduced the sensitivity to  $\beta$ -adrenergic stimulation *in vitro* and *in vivo*. Our findings shed light on the epigenetic control of  $\beta$ -adrenergic responses via TET–HDAC cooperation. Because loss of TET proteins in adipocytes robustly defended against the suppressive effects of chronic overnutrition on  $\beta$ -adrenergic sensitivity, thermogenesis, and energy expenditure, targeting the TET–HDAC– $\beta$ 3-AR axis may increase therapeutic options for treating obesity and related metabolic diseases.

## Materials and Methods

Mice carrying *LoxP*-targeted (floxed) *Tet1<sup>fl/fl</sup>*, *Tet2<sup>fl/fl</sup>*, and *Tet3<sup>fl/fl</sup>* have been described previously (76–78) and were provided by Dr. Anjana Rao (La Jolla Institute, CA, USA). *Adiponectin-Cre* (#010803) and *Cre-ERT2* (#8085) transgenic mice were obtained from the Jackson Laboratory. Detailed materials and methods can be found in *SI Appendix*, *SI Materials and Methods*.

**Data Availability.** RNA-sequencing datasets used in this study have been deposited in National Center for Biotechnology Information (NCBI) Gene Expression Omnibus (GEO) repository with the accession number [GSE178762](https://www.ncbi.nlm.nih.gov/geo/query/acc.cgi?acc=GSE178762).

**ACKNOWLEDGMENTS.** This work was supported by the National Research Foundation of Korea (Grants 2018R1D1A1B07049676, 2019R1F1A1063340, 2018R1A6A1A03025810, and 2017R1C1B2005604) and the Future-leading Project Research Fund of Ulsan National Institute of Science and Technology (Grant 1.220023.01). M.K. is also supported by the Center for Genomic Integrity, Institute for Basic Science (Grant IBS-R022-D1).

Author affiliations: <sup>a</sup>Department of Biological Sciences, Ulsan National Institute of Science and Technology, Ulsan 44919, Republic of Korea; <sup>b</sup>Department of Life Sciences, Jeonbuk National University, Jeonju 54896, Republic of Korea; <sup>c</sup>Department of Biomedical Engineering, Ulsan National Institute of Science and Technology, Ulsan 44919, Republic of Korea; and <sup>d</sup>Center for Genomic Integrity, Institute for Basic Science, Ulsan 44919, Republic of Korea

1. J. Robidoux, T. L. Martin, S. Collins, Beta-adrenergic receptors and regulation of energy expenditure: A family affair. *Annu. Rev. Pharmacol. Toxicol.* **44**, 297–323 (2004).
2. B. A. Evans, J. Merlin, T. Bengtsson, D. S. Hutchinson, Adrenoceptors in white, brown, and brite adipocytes. *Br. J. Pharmacol.* **176**, 2416–2432 (2019).
3. E. T. Chouchani, S. Kajimura, Metabolic adaptation and maladaptation in adipose tissue. *Nat. Metab.* **1**, 189–200 (2019).
4. B. Lowell, B. M. Spiegelman, Towards a molecular understanding of adaptive thermogenesis. *Nature* **404**, 652–660 (2000).
5. A. Fedorenko, P. V. Lishko, Y. Kirichok, Mechanism of fatty-acid-dependent UCP1 uncoupling in brown fat mitochondria. *Cell* **151**, 400–413 (2012).
6. Y. Jiang, D. C. Berry, J. M. Graff, Distinct cellular and molecular mechanisms for  $\beta$ 3 adrenergic receptor-induced beige adipocyte formation. *eLife* **6**, e30329 (2017).
7. C. Cero *et al.*,  $\beta$ 3-Adrenergic receptors regulate human brown/beige adipocyte lipolysis and thermogenesis. *JCI Insight* **6**, e139160 (2021).
8. M. Ghorbani, S. Teimourian, R. Farzad, N. N. Asl, Apparent histological changes of adipocytes after treatment with CL 316,243, a  $\beta$ 3-adrenergic receptor agonist. *Drug Des. Devel. Ther.* **9**, 669–676 (2015).
9. E. Widén *et al.*, Association of a polymorphism in the beta 3-adrenergic-receptor gene with features of the insulin resistance syndrome in Finns. *N. Engl. J. Med.* **333**, 348–351 (1995).
10. K. Clément *et al.*, Genetic variation in the beta 3-adrenergic receptor and an increased capacity to gain weight in patients with morbid obesity. *N. Engl. J. Med.* **333**, 352–354 (1995).
11. E. S. Bachman *et al.*, betaAR signaling required for diet-induced thermogenesis and obesity resistance. *Science* **297**, 843–845 (2002).
12. V. S. Susulic *et al.*, Targeted disruption of the beta 3-adrenergic receptor gene. *J. Biol. Chem.* **270**, 29483–29492 (1995).
13. S. Reynisdottir, K. Ellerfeldt, H. Wahrenberg, H. Lithell, P. Arner, Multiple lipolysis defects in the insulin resistance (metabolic) syndrome. *J. Clin. Invest.* **93**, 2590–2599 (1994).
14. J. W. Jocken, E. E. Blaak, C. J. van der Kallen, M. A. van Baak, W. H. Saris, Blunted beta-adrenoceptor-mediated fat oxidation in overweight subjects: A role for the hormone-sensitive lipase gene. *Metabolism* **57**, 326–332 (2008).
15. T. Guo *et al.*, Adipocyte ALK7 links nutrient overload to catecholamine resistance in obesity. *eLife* **3**, e03245 (2014).

16. S. Collins *et al.*, Impaired expression and functional activity of the beta 3- and beta 1-adrenergic receptors in adipose tissue of congenitally obese (C57BL/6J ob/ob) mice. *Mol. Endocrinol.* **8**, 518–527 (1994).
17. P. Muzzin *et al.*, An adipose tissue-specific beta-adrenergic receptor. Molecular cloning and down-regulation in obesity. *J. Biol. Chem.* **266**, 24053–24058 (1991).
18. S. Collins, K. W. Daniel, E. M. Rohfs, Depressed expression of adipocyte beta-adrenergic receptors is a common feature of congenital and diet-induced obesity in rodents. *Int. J. Obes. Relat. Metab. Disord.* **23**, 669–677 (1999).
19. R. De Matteis *et al.*, Immunohistochemical identification of the beta(3)-adrenoceptor in intact human adipocytes and ventricular myocardium: Effect of obesity and treatment with ephedrine and caffeine. *Int. J. Obes. Relat. Metab. Disord.* **26**, 1442–1450 (2002).
20. S. K. Shenoy *et al.*, beta-arrestin-dependent, G protein-independent ERK1/2 activation by the beta2 adrenergic receptor. *J. Biol. Chem.* **281**, 1261–1273 (2006).
21. T. T. Cao, H. W. Deacon, D. Reczek, A. Bretscher, M. von Zaastrow, A kinase-regulated PDZ-domain interaction controls endocytic sorting of the beta2-adrenergic receptor. *Nature* **401**, 286–290 (1999).
22. M. Ghorbani, T. H. Claus, J. Himms-Hagen, Hypertrophy of brown adipocytes in brown and white adipose tissues and reversal of diet-induced obesity in rats treated with a beta3-adrenoceptor agonist. *Biochem. Pharmacol.* **54**, 121–131 (1997).
23. J. G. Granneman, P. Li, Z. Zhu, Y. Lu, Metabolic and cellular plasticity in white adipose tissue I: Effects of beta3-adrenergic receptor activation. *Am. J. Physiol. Endocrinol. Metab.* **289**, E608–E616 (2005).
24. X. Liu, F. Pérusse, L. J. Bukowiecki, Mechanisms of the antidiabetic effects of the beta 3-adrenergic agonist CL-316243 in obese Zucker-ZDF rats. *Am. J. Physiol.* **274**, R1212–R1219 (1998).
25. L. Hao *et al.*, Beneficial metabolic effects of mirabegron in vitro and in high-fat diet-induced obese mice. *J. Pharmacol. Exp. Ther.* **369**, 419–427 (2019).
26. J. R. Arch *et al.*, Atypical beta-adrenoceptor on brown adipocytes as target for anti-obesity drugs. *Nature* **309**, 163–165 (1984).
27. J. R. Arch, Challenges in  $\beta$ (3)-adrenoceptor agonist drug development. *Ther. Adv. Endocrinol. Metab.* **2**, 59–64 (2011).
28. B. S. Finlin *et al.*, The  $\beta$ 3-adrenergic receptor agonist mirabegron improves glucose homeostasis in obese humans. *J. Clin. Invest.* **130**, 2319–2331 (2020).
29. B. S. Finlin *et al.*, Human adipose beiging in response to cold and mirabegron. *JCI Insight* **3**, e121510 (2018).
30. A. E. O'Mara *et al.*, Chronic mirabegron treatment increases human brown fat, HDL cholesterol, and insulin sensitivity. *J. Clin. Invest.* **130**, 2209–2219 (2020).
31. A. M. Cypess *et al.*, Activation of human brown adipose tissue by a  $\beta$ 3-adrenergic receptor agonist. *Cell Metab.* **21**, 33–38 (2015).
32. W. A. Pastor, L. Aravind, A. Rao, TETonic shift: Biological roles of TET proteins in DNA demethylation and transcription. *Nat. Rev. Mol. Cell Biol.* **14**, 341–356 (2013).
33. H. Wu *et al.*, Dual functions of Tet1 in transcriptional regulation in mouse embryonic stem cells. *Nature* **473**, 389–393 (2011).
34. G. C. Hon *et al.*, 5mC oxidation by Tet2 modulates enhancer activity and timing of transcriptome reprogramming during differentiation. *Mol. Cell* **56**, 286–297 (2014).
35. A. Tsagaratou *et al.*, Dissecting the dynamic changes of 5-hydroxymethylcytosine in T-cell development and differentiation. *Proc. Natl. Acad. Sci. U.S.A.* **111**, E3306–E3315 (2014).
36. X. Wu, G. Li, R. Xie, Decoding the role of TET family dioxygenases in lineage specification. *Epigenetics Chromatin* **11**, 58 (2018).
37. K. Williams *et al.*, TET1 and hydroxymethylcytosine in transcription and DNA methylation fidelity. *Nature* **473**, 343–348 (2011).
38. Q. Zhang *et al.*, Tet2 is required to resolve inflammation by recruiting Hdac2 to specifically repress IL-6. *Nature* **525**, 389–393 (2015).
39. S. Damal Villivalam *et al.*, TET1 is a beige adipocyte-selective epigenetic suppressor of thermogenesis. *Nat. Commun.* **11**, 4313 (2020).
40. K. Fujiki *et al.*, PPAR $\gamma$ -induced PARylation promotes local DNA demethylation by production of 5-hydroxymethylcytosine. *Nat. Commun.* **4**, 2262 (2013).
41. L. Wihle *et al.*, Tet1 and Tet2 protect DNA methylation canyons against hypermethylation. *Mol. Cell. Biol.* **36**, 452–461 (2015).
42. Y. Yuan *et al.*, Vitamin C inhibits the metabolic changes induced by tet1 insufficiency under high fat diet stress. *Mol. Nutr. Food Res.* **65**, e2100417 (2021).
43. Y. Huang *et al.*, The behaviour of 5-hydroxymethylcytosine in bisulfite sequencing. *PLoS One* **5**, e8888 (2010).
44. S. Herzig *et al.*, CREB regulates hepatic gluconeogenesis through the coactivator PGC-1. *Nature* **413**, 179–183 (2001).
45. C. W. Lio *et al.*, Tet2 and Tet3 cooperate with B-lineage transcription factors to regulate DNA modification and chromatin accessibility. *eLife* **5**, e18290 (2016).
46. S. Montagner *et al.*, TET2 regulates mast cell differentiation and proliferation through catalytic and non-catalytic activities. *Cell Rep.* **15**, 1566–1579 (2016).
47. Y. Bao *et al.*, DNA demethylase Tet2 suppresses cisplatin-induced acute kidney injury. *Cell Death Discov.* **7**, 167 (2021).
48. J. Eguchi *et al.*, Transcriptional control of adipose lipid handling by IRF4. *Cell Metab.* **13**, 249–259 (2011).
49. J. An *et al.*, Acute loss of TET function results in aggressive myeloid cancer in mice. *Nat. Commun.* **6**, 10071 (2015).
50. M. M. Dawlaty *et al.*, Combined deficiency of Tet1 and Tet2 causes epigenetic abnormalities but is compatible with postnatal development. *Dev. Cell* **24**, 310–323 (2013).
51. R. T. Jung, P. S. Shetty, W. P. James, M. A. Barrand, B. A. Callingham, Reduced thermogenesis in obesity. *Nature* **279**, 322–323 (1979).
52. J. R. Speakman, Measuring energy metabolism in the mouse - Theoretical, practical, and analytical considerations. *Front. Physiol.* **4**, 34 (2013).
53. T. D. Müller, M. Klingenspor, M. H. Tschöp, Revisiting energy expenditure: How to correct mouse metabolic rate for body mass. *Nat. Metab.* **3**, 1134–1136 (2021).
54. J. Lin, C. Handschin, B. M. Spiegelman, Metabolic control through the PGC-1 family of transcription coactivators. *Cell Metab.* **1**, 361–370 (2005).
55. J. van der Vlag, J. L. den Blaauwen, R. G. Sewalt, R. van Driel, A. P. Otte, Transcriptional repression mediated by polycomb group proteins and other chromatin-associated repressors is selectively blocked by insulators. *J. Biol. Chem.* **275**, 697–704 (2000).
56. R. Liu *et al.*, Regulation of CSF1 promoter by the SWI/SNF-like BAF complex. *Cell* **106**, 309–318 (2001).
57. J. E. Moore *et al.*; ENCODE Project Consortium, Expanded encyclopaedias of DNA elements in the human and mouse genomes. *Nature* **583**, 699–710 (2020).
58. A. A. Sérandour *et al.*, Dynamic hydroxymethylation of deoxyribonucleic acid marks differentiation-associated enhancers. *Nucleic Acids Res.* **40**, 8255–8265 (2012).
59. E. Jeffery *et al.*, Characterization of Cre recombinase models for the study of adipose tissue. *Adipocyte* **3**, 206–211 (2014).
60. B. X. Ong *et al.*, Regulation of thermogenic adipocyte differentiation and adaptive thermogenesis through histone acetylation. *Front. Endocrinol. (Lausanne)* **11**, 95 (2020).
61. A. Galmozzi *et al.*, Inhibition of class I histone deacetylases unveils a mitochondrial signature and enhances oxidative metabolism in skeletal muscle and adipose tissue. *Diabetes* **62**, 732–742 (2013).
62. A. Ferrari *et al.*, HDAC3 is a molecular brake of the metabolic switch supporting white adipose tissue browning. *Nat. Commun.* **8**, 93 (2017).
63. F. Li *et al.*, Histone deacetylase 1 (HDAC1) negatively regulates thermogenic program in brown adipocytes via coordinated regulation of histone H3 lysine 27 (H3K27) deacetylation and methylation. *J. Biol. Chem.* **291**, 4523–4536 (2016).
64. Z. Gao *et al.*, Butyrate improves insulin sensitivity and increases energy expenditure in mice. *Diabetes* **58**, 1509–1517 (2009).
65. H. Xu *et al.*, Chronic inflammation in fat plays a crucial role in the development of obesity-related insulin resistance. *J. Clin. Invest.* **112**, 1821–1830 (2003).
66. C. Deng *et al.*, Respective degree of expression of beta 1-, beta 2- and beta 3-adrenoceptors in human brown and white adipose tissues. *Br. J. Pharmacol.* **118**, 929–934 (1996).
67. N. Dhillwyo, M. P. Sarras Jr., E. Luczkowski, S. M. Mason, R. V. Intine, Parp inhibition prevents ten-eleven translocase enzyme activation and hyperglycemia-induced DNA demethylation. *Diabetes* **63**, 3069–3076 (2014).
68. E. F. Yuan *et al.*, Hyperglycemia affects global 5-methylcytosine and 5-hydroxymethylcytosine in blood genomic DNA through upregulation of SIRT6 and TETs. *Clin. Epigenetics* **11**, 63 (2019).
69. D. Wu *et al.*, Glucose-regulated phosphorylation of TET2 by AMPK reveals a pathway linking diabetes to cancer. *Nature* **559**, 637–641 (2018).
70. M. M. Ali, S. A. Phillips, A. M. Mahmoud, HIF1 $\alpha$ /TET1 pathway mediates hypoxia-induced adipocytokine promoter hypomethylation in human adipocytes. *Cells* **9**, 134 (2020).
71. J. Z. Cao, H. Liu, A. Wickrema, L. A. Godley, HIF-1 directly induces TET3 expression to enhance 5-hmC density and induce erythroid gene expression in hypoxia. *Blood Adv.* **4**, 3053–3062 (2020).
72. R. Matuleviciute, P. P. Cunha, R. S. Johnson, I. P. Foskolou, Oxygen regulation of TET enzymes. *FEBS J.* **288**, 7143–7161 (2021).
73. Y. S. Lee *et al.*, Increased adipocyte O<sub>2</sub> consumption triggers HIF-1 $\alpha$ , causing inflammation and insulin resistance in obesity. *Cell* **157**, 1339–1352 (2014).
74. J. Krishnan *et al.*, Dietary obesity-associated Hif1 $\alpha$  activation in adipocytes restricts fatty acid oxidation and energy expenditure via suppression of the Sirt2-NAD<sup>+</sup> system. *Genes Dev.* **26**, 259–270 (2012).
75. C. Jiang *et al.*, Disruption of hypoxia-inducible factor 1 in adipocytes improves insulin sensitivity and decreases adiposity in high-fat diet-fed mice. *Diabetes* **60**, 2484–2495 (2011).
76. M. Ko *et al.*, Ten-eleven-translocation 2 (TET2) negatively regulates homeostasis and differentiation of hematopoietic stem cells in mice. *Proc. Natl. Acad. Sci. U.S.A.* **108**, 14566–14571 (2011).
77. M. Ko *et al.*, TET proteins and 5-methylcytosine oxidation in hematological cancers. *Immunol. Rev.* **263**, 6–21 (2015).
78. J. Kang *et al.*, Simultaneous deletion of the methylcytosine oxidases Tet1 and Tet3 increases transcriptome variability in early embryogenesis. *Proc. Natl. Acad. Sci. U.S.A.* **112**, E4236–E4245 (2015).